Electronic and Optical Properties of Rare Earth Oxides: *Ab Initio* Calculation

Sezen Horoz[1], Sevket Simsek[2], Selami Palaz[3], Amirullah M. Mamedov[4,5*]

[1]Institute of Natural Sciences, Cukurova University, Adana, Turkey
[2]Department of Material Science and Engineering, Hakkari University, Hakkari, Turkey
[3]Department of Physics, Faculty of Science and Letters, Harran University, Sanliurfa, Turkey
[4]Nanotechnology Research Center (NANOTAM), Bilkent University, Ankara, Turkey
[5]International Scientific Center, Baku State University, Baku, Azerbaijan
Email: [*]mamedov@bilkent.edu.tr

Abstract

In this work, we have investigated the electronic and optical properties of the technologically important rare earth oxide compounds—X_2O_3 (X: Gd, Tb) using the density functional theory within the GGA. The band structure of X_2O_3 have been calculated along high symmetry directions in the first brillouin zone. The real and imaginary parts of dilectric functions and the other optical responses such as energy-loss function, the effective number of valence electrons and the effective optical dielectric constants of the rare earth sesquioxides (Gd_2O_3 and Tb_2O_3) were calculated.

1. Introduction

X_2O_3 (X:Gd, Tb) are the interesting materials from both fundamental and industrial perspectives and have a wide range of applications. They are thermodynamically stable, making them useful for corrosion resistive coating [1]-[5]. Additionally, their high refractive indices lead to applications in optics, such as antireflection coatings, switches, filters and modulators [1] [4]. The most recent interest of them is due to their high dielectric constants and electrical stability, making them good candidates for a new class of gate oxides in metal-oxide semiconductor field-effect transistors [1]. In addition, many properties of rare-earth sesquioxides are determined by their semicore *f*-levels. While being mainly localized on the rare-earth atoms and usually not participating in

[*]Corresponding author.

bonding and electronic conduction, *f*-shell electrons are available for optical transition and can establish strong magnetic order [1]. So far as we know, no *ab initio* general potential calculation of the optical properties of the rare-earth sesquioxides has been reported. The main purpose of this work is to provide some additional information to the existing features of Gd_2O_3 and Tb_2O_3 by using density functional theory. Therefore, in this work, we have investigated the electronic and optical properties of Gd_2O_3 and Tb_2O_3 compounds.

2. Method of Calculation

In the present paper, all calculations have been carried out using the *ab-initio* total-energy and molecular-dynamics program VASP (Vienna *ab-initio* simulation program) developed at the Faculty of Physics of the University of Vienna [6]-[9] within the density functional theory (DFT) [10]. The exchange-correlation energy function is treated within the GGA (generalized gradient approximation) by the density functional of Perdew *et al.* [11]. We get a good convergence using a $5 \times 5 \times 5$ Monkhorst-Pack [12] mesh grid for the total-energy calculation with a cutoff energy of 510 eV for both compunds. The electronic iterations convergence is 1.0×10^{-5} eV using the Normal (blocked Davidson) algorithm and reciprocal space projection operators. These values were found to be sufficient for studying the electronic and optical properties of X_2O_3 crystals.

3. Results and Discussion

3.1. Structural and Electronic Properties

In the first step of our calculations, we have carried out the equilibrium lattice constants of Gd_2O_3, and Tb_2O_3 by minimizing the ratio of the total energy of the crystal to its volume using the experimental data [13] [15]. We have compared the present results for lattice parameters of X_2O_3 with previous experimental values [13]-[29] and are given in **Table 1**. These results are within the accuracy range of calculations based on density functional theory.

Table 1. The calculatedequilibriumlattice parameters and direct band gaps together with the available experimental values for Gd_2O_3 and Tb_2O_3.

| Material	Reference	a = b = c (Å)	E_g (eV)	Space Group
Gd_2O_3	Present (GGA-VASP)	10.817	3.86	$Ia3(No:206)$
	Ref. [13]	10.815		
	Ref. [14]	10.78		
	Ref. [15]	10.816		
	Ref. [16]	10.817		
	Ref. [17]	10.812		
	Ref. [18]	10.808		
	Ref. [19]	10.819		
	Ref. [20]	10.817		
	Ref. [21]	10.817		
Tb_2O_3	Present (GGA-VASP)	10.758	3.82	$Ia3(No:206)$
	Ref. [15]	10.758		
	Ref. [22]	10.7		
	Ref. [23]	10.745		
	Ref. [24]	10.7		
	Ref. [25]	10.735		
	Ref. [26]	10.728		
	Ref. [27]	10.73		
	Ref. [28]	10.728		

The investigation of electronic band structure for understanding the electronic and optical properties of X_2O_3 is very useful. The band structures of the X_2O_3 were calculated using GGA. The electronic band structures were calculated along the special lines connecting the high-symmetry points Γ, H, N, and P for X_2O_3 in the k-space. The electronic band structure of Gd_2O_3, and Tb_2O_3 along the high symmetry directions have been calculated by using the equilibrium lattice constants and are given in **Figure 1** and **Figure 2**.

As can be seen in **Figure 1**, the Gd_2O_3 compound has a direct band gap semiconductor with the value 3.86 eV (in Γ-high symmetry point). The band gap with the value 3.82 eV of Tb_2O_3 compound has the same character of that of Gd_2O_3 (**Figure 2**). The band gap values obtained for X_2O_3 are good agreement with the earlier theoretical resuts, but is less than the estimated experimental results [1] [3] [5]. In these figures (**Figure 1** and **Figure 2**), the lowest valance bands that occur between 0 and −3.5 eV (72 energy states) are dominated by O 2p states while the valence bands that occur between −14 eV and −16.5 eV (24 energy states) are dominated by Gd 6s and Tb 6s states. The lowest occupied valance bands are essentially dominated by O 2s (−19 eV and −21.5 eV and include 48 energy states).

3.2. Optical Properties

It is well known that the effect of the electric field vector, $E(\omega)$, of the incoming light is to polarize the material. At the level of a linear response, this polarization can be calculated using the following relation [29]:
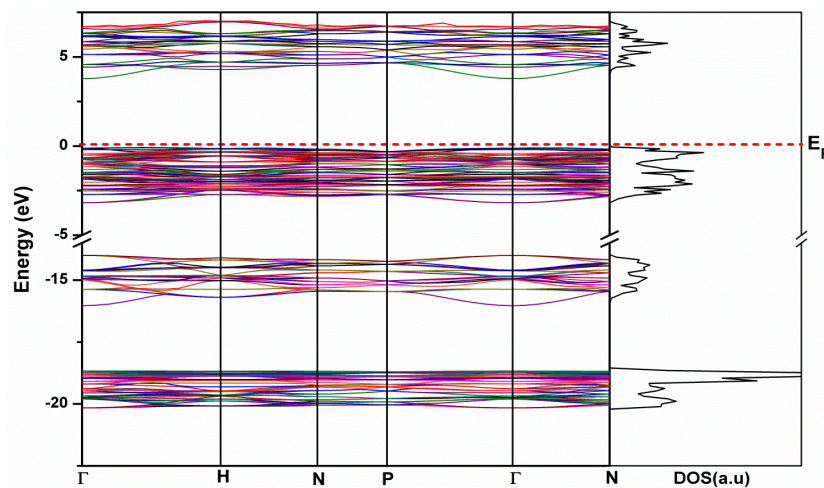
Figure 1. The calculated electronic band structure and Density of State for Gd_2O_3.
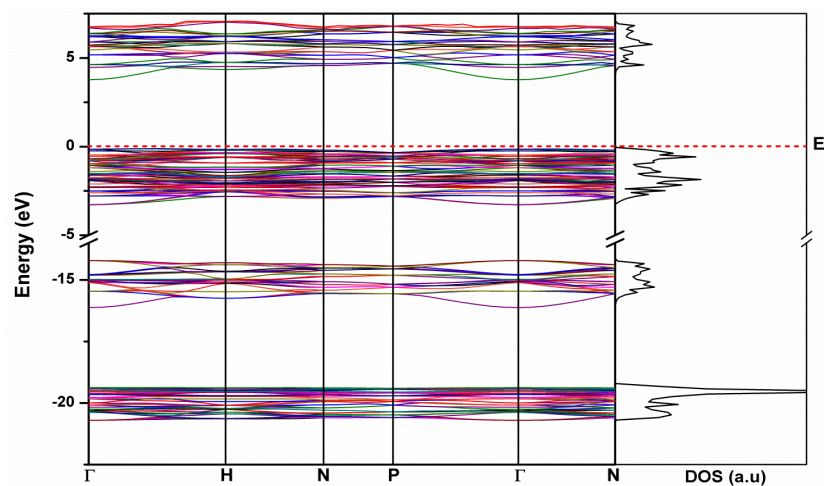
Figure 2. The calculated electronic band structure Density of State for Tb_2O_3.

$$P^i(\omega) = \chi^{(1)}_{ij}(-\omega, \omega) E^j(\omega) \tag{1}$$

where $\chi^{(1)}_{ij}$ is the linear optical susceptibility tensor and it is given by [30]

$$\chi^{(1)}_{ij}(-\omega, \omega) = \frac{e^2}{\hbar\Omega} \sum_{nmk} f_{nm}(k) \frac{r^i_{nm}(k) r^i_{mn}(k)}{\omega_{mn}(k) - \omega} = \frac{\varepsilon_{ij}(\omega) - \delta_{ij}}{4\pi} \tag{2}$$

where n, m denote energy bands, $f_{mn}(k) \equiv f_m(k) - f_n(k)$ is the Fermi occupation factor, Ω is the normalization volume. $\omega_{mn}(k) \equiv \omega_m(k) - \omega(k)$ are the frequency differences, $\hbar\omega_n(k)$ is the energy of band n at wave vector k. The r_{nm} are the matrix elements of the position operator [30].

As can be seen in Equation (2), the dielectric function $\varepsilon_{ij}(\omega) = 1 + 4\pi\chi^{(1)}_{ij}(-\omega, \omega)$ and the imaginary part of $\varepsilon_{ij}(\omega)$, $\varepsilon^{ij}_2(\omega)$ is given by

$$\varepsilon^{ij}_2(\omega) = \frac{e^2}{\hbar\pi} \sum_{nm} \int dk \, f_{nm}(k) \frac{v^i_{nm}(k) v^j_{nm}(k)}{\omega^2_{mn}} \delta(\omega - \omega_{mn}(k)) \tag{3}$$

The real part of $\varepsilon_{ij}(\omega)$, $\varepsilon^{ij}_1(\omega)$, can be obtained by using the Kramers-Kroning transformation [30]. Because the Kohn-Sham equations determine the ground state properties, the unoccupied conduction bands as calculated, have no physical significance.

The known sum rules [30] can be used to determine some quantitative parameters, particularly the effective number of the valence electrons per unit cell N_{eff}, as well as the effective optical dielectric constant ε_{eff}, which make a contribution to the optical constants of a crystal at the energy E_0. One can obtain an estimate of the distribution of oscillator strengths for both intraband and interband transitions by computing the $N_{eff}(E_0)$ defined according to

$$N_{eff}(E) = \frac{2m\varepsilon_0}{\pi\hbar^2 e^2 N_a} \int_0^\infty \varepsilon_2(E) E dE \tag{4}$$

where N_a is the density of atoms in a crystal, e and m are the charge and mass of the electron, respectively, and $N_{eff}(E_0)$ is the effective number of electrons contributing to optical transitions below an energy of E_0.

Further information on the role of the core and semi-core bands may be obtained by computing the contribution that the various bands make to the static dielectric constant, ε_0. According to the Kramers-Kronig relations, one has

$$\varepsilon_0(E) - 1 = \frac{2}{\pi} \int_0^\infty \varepsilon_2(E) E^{-1} dE \tag{5}$$

One can therefore define an "effective" dielectric constant, that represents a different mean of the interband transitions from that represented by the sum rule, Equation (5), according to the relation

$$\varepsilon_{eff}(E) - 1 = \frac{2}{\pi} \int_0^{E_0} \varepsilon_2(E) E^{-1} dE \tag{6}$$

The physical meaning of ε_{eff} is quite clear: ε_{eff} is the effective optical dielectric constant governed by the interband transitions in the energy range from zero to E_0, *i.e.* by the polarization of the electron shells.

We first calculated the real and imaginary parts of the linear dielectric function of the Gd_2O_3, and Tb_2O_3 compounds (**Figure 3** and **Figure 4**). In order to calculate the optical response by using the calculated band structure, we have chosen a photon energy range of 0 - 65 eV and have seen that a 0 - 40 eV photon energy range is sufficient for most optical functions. We first calculated the real and imaginary parts of linear dielectric function of the Gd_2O_3 and Tb_2O_3 compounds (**Figure 4** and **Figure 5**). All the Gd_2O_3 and Tb_2O_3 compounds
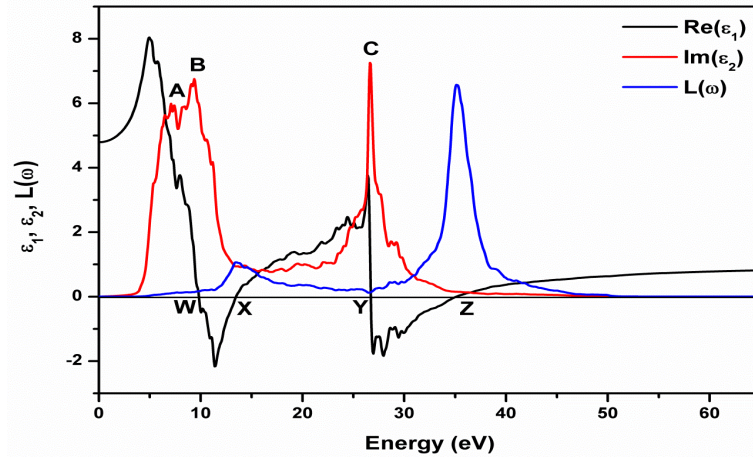
Figure 3. The real and imaginary parts of the linear dielectric function and Electron energy-loss spectrum of Gd_2O_3.
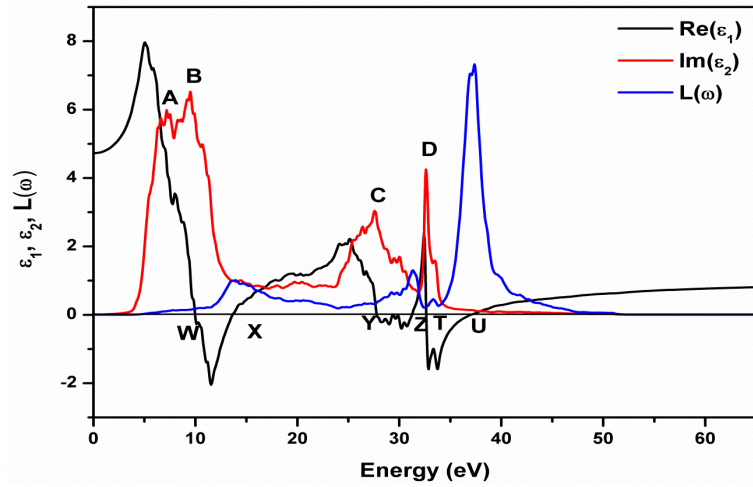
Figure 4. The real and imaginary parts of the linear dielectric function and Electron energy-loss spectrum of Tb_2O_3.

studied so far have ε_1 are equal to zero in the energy region between 9 eV and 40 eV for decreasing $(d\varepsilon_1/dE < 0)$ and increasing of $(d\varepsilon_1/dE > 0)\,\varepsilon_1$ (see, **Table 2**). Also, values of ε_1 versus photon energy have main peaks in the energy region 4 eV and 30 eV. Some of the principal features and singularities of the ε_{ij} for both investigated compounds are shown in **Table 3**.

The peaks of the correspond to the optical transitions from the valence band to the conduction band and are in agreement with the previous results. The maximum peak values of ε_2 for Gd_2O_3 and Tb_2O_3 are around 9.31 eV and 9.49 eV, respectively.

The corresponding energy-loss functions, $L(\omega)$, were calculated using Equation (7) and are also presented in **Figure 3** and **Figure 4**. The $L(\omega)$ describes the energy loss of fast electrons traversing the material. The sharp maxima in the energy loss function are associated with the existence of plasma oscillations [30]. The curves of L have a maximum near 35 eV (Gd_2O_3) and 38 eV (Tb_2O_3).

$$L(\omega) = \frac{\varepsilon_2(\omega)}{\varepsilon_1^2(\omega) + \varepsilon_2^2(\omega)} \qquad (7)$$

The calculated effective number of valence electrons N_{eff} is given in **Figure 5(a)**. The effective number of valence electron per unit cell, N_{eff} up to 5 eV is zero (below the band gap) then reaches saturation values at
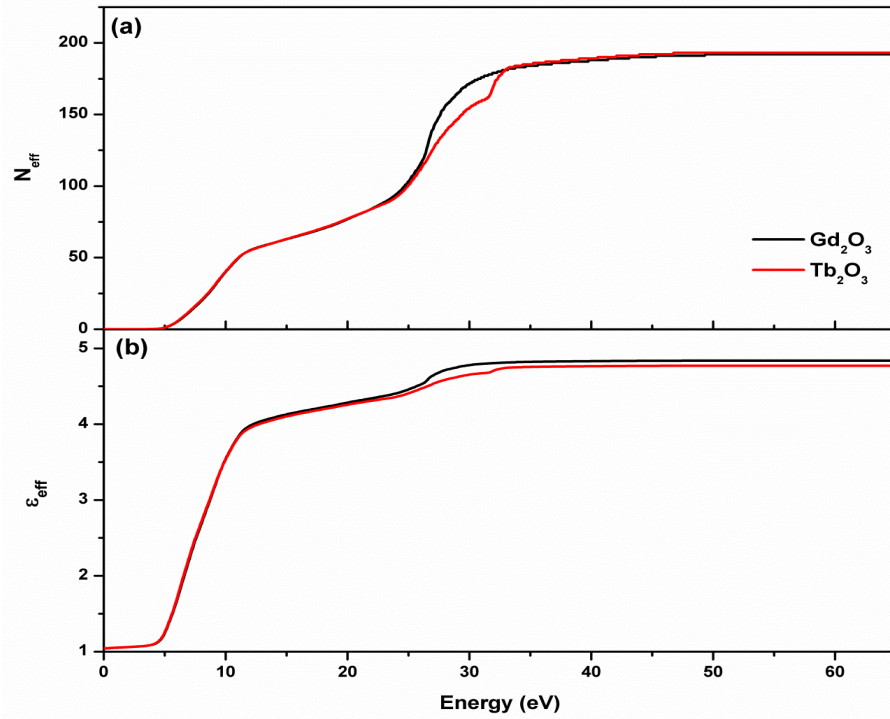
Figure 5. The calculated (a) effective number of electrons participating in the interband transitions and (b) effective optical dielectric constant.

Table 2. The energy values at the zero point of real part of dielectric function for Gd_2O_3 and Tb_2O_3.

	zero points (eV)					
Crystal	W	X	Y	Z	T	U
Gd_2O_3	9.676	13.446	26.574	35.023		
Tb_2O_3	10.039	13.628	27.830	31.419	32.494	36.628

Table 3. The maximum peak values of the imaginary part of the dielectric function for Gd_2O_3 and Tb_2O_3.

	maximum peak values (eV)			
Crystal	A	B	C	D
Gd_2O_3	6.9803	9.3121	26.574	
Tb_2O_3	7.328	9.494	27.648	32.676

about 30 eV (Gd_2O_3) and 35 eV (Tb_2O_3). This means that deep-lying valence orbitals participate in the interband transitiond as well (see **Figure 1** and **Figure 2**). The effective optical dielectric constant, ε_{eff}, is shown in **Figure 5(b)**.

The curves of ε_{eff} can be arbitrarily divided into two parts. The first part is characterized by a rapid growth of ε_{eff} and extends up to 12 eV. The second part shows a smoother and slower growth of ε_{eff} and reaches a saturation values at about 30 eV(Gd_2O_3) and 35 eV (Tb_2O_3). This means that the largest contribution to ε_{eff} is made by transitions corresponding to the bands at ~5 eV and ~12 eV.

4. Conclusion

In the present work, we have made a detailed investigation of the electronic, and frequency-dependent linear optical properties of the X_2O_3 (X: Gd and Tb) crystals using the density functional methods. The result of the structural optimization implemented using the GGA are in good agreement with the experimental and theoretical

results. We have examined photon-energy dependent dielectric functions, some optical properties such as the energy-loss function, the effective number of valance electrons and the effective optical dielectric constants for both materials.

Acknowledgements

References

[1] Adachi, G., Imanaka, N. and Kang, Z.C. (2004) Binary Rare Earth Oxides. Kluwer Academic Publishers, New York.

[2] Frank, G., Tatsuro, W. and Wolfgang, B. (2010) Rare Earth oxide Alloys and Stacked Layers: An *ab Initio* Study. *Thin Solid Films*, **518**, 4747-4749. http://dx.doi.org/10.1016/j.tsf.2009.12.074

[3] Gerald, L. (2006) Band Edge Electronic Structure of Transition Metal/Rare Earth Oxide Dielectrics. *Applied Surface Science*, **253**, 311-321. http://dx.doi.org/10.1016/j.apsusc.2006.06.001

[4] Wang, J.J., Ji, T., Zhu, Y.Y., Fang, Z.B. and Ren, W.Y. (2012) Band Gap and Structure Characterization of Tm_2O_3 Films. *Journal of Rare Earths*, **30**, 233-235. http://dx.doi.org/10.1016/S1002-0721(12)60029-5

[5] Roland, G., Stewart, J.C. and John, R. (2013) Nature of the Electronic Band Gap in Lanthanide Oxides. *Physical Review B*, **87**, 125116-125122. http://dx.doi.org/10.1103/PhysRevB.87.125116

[6] Kresse, G. and Hafner, J. (1993) *Ab Initio* Molecular Dynamics for Liquid Metals. *Physical Review B*, **47**, 558-561. http://dx.doi.org/10.1103/PhysRevB.47.558

[7] Kresse, G. and Furthmüller, J. (1996) Efficiency of *Ab-Initio* Total Energy Calculations for Metals and Semiconductors Using a Plane-Wave Basis Set. *Computational Materials Science*, **6**, 15-50. http://dx.doi.org/10.1016/0927-0256(96)00008-0

[8] Kresse, G. and Joubert, D. (1999) From Ultrasoft Pseudopotentials to the Projector Augmented-Wave Method. *Physical Review B*, **59**, 1758-1775. http://dx.doi.org/10.1103/PhysRevB.59.1758

[9] Kresse, G. and Furthmüller, J. (1996) Efficient Iterative Schemes for *ab Initio* Total-Energy Calculations Using a Plane-Wave Basis Set. *Physical Review B*, **54**, 11169-11186. http://dx.doi.org/10.1103/PhysRevB.54.11169

[10] Hohenberg, P. and Kohn, W. (1964) Inhomogeneous Electron Gas. *Physical Review*, **136**, B864-B871. http://dx.doi.org/10.1103/physrev.136.b864

[11] Perdew, J.P., Burke, S. and Ernzerhof, M. (1996) Generalized Gradient Approximation Made Simple. *Physical Review Letters*, **77**, 3865-3868. http://dx.doi.org/10.1103/PhysRevLett.77.3865

[12] Monkhorst, H.J. and Pack, J.D. (1976) Special Points for Brillouin-Zone Integrations. *Physical Review B*, **13**, 5188-5192. http://dx.doi.org/10.1103/PhysRevB.13.5188

[13] Bartos, A., Lieb, K.P., Uhrmacher, M. and Wiarda, D. (1993) Refinement of Atomic Positions in Bixbyite Oxides Using Perturbed Angular Correlation Spectroscopy. *Acta Crystallographica Section B Structural Science*, **49**, 165-169. http://dx.doi.org/10.1107/S0108768192007742

[14] Post, B., Moskowitz, D. and Glaser, F.W. (1956) Borides of Rare Earth Metals. *Journal of the American Chemical Society*, **78**, 1800-1802. http://dx.doi.org/10.1021/ja01590a007

[15] Andreeva, A.F. and Gil'man, I.Y. (1978) Polymorphic Transitions in Rare Earth Oxides Obtained by Reactive Evaporation. *Inorganic Materials*, **14**, 384-390. (İn Russian)

[16] Adachi, G.Y., Kawahito, T., Matsumoto, H. and Shiokawa, J. (1970) The Reactions of Lanthanide Oxides and Antimony Oxides. *Journal of Inorganic and Nuclear Chemistry*, **32**, 681-686. http://dx.doi.org/10.1016/0022-1902(70)80278-0

[17] Hirosaki, N., Ogata, S. and Kocer, C. (2003) *Ab İnitio* Calculation of the Crystal Structure of the Lanthanide Ln_2O_3 Sesquioxides. *Journal of Alloys and Compounds*, **351**, 31-34. http://dx.doi.org/10.1016/S0925-8388(02)01043-5

[18] Scavini, M., Coduri, M., Allieta, M., Brunelli, M. and Ferrero, C. (2012) Probing Complex Disorder in $Ce_{1-x}Gd_xO_{2-x/2}$ Using the Pair Distribution Function Analysis. *Chemistry of Materials*, **24**, 1338-1345. http://dx.doi.org/10.1021/cm203819u

[19] Zhang, F.X., Lang, M., Wang, W., Becker, U. and Ewing, R.C. (2008) Structural Phase Transitions of Cubic Gd_2O_3 at High Pressures. *Physical Review B*, **78**, Article ID: 064114. http://dx.doi.org/10.1103/PhysRevB.78.064114

[20] Pires, A.M., Davolos, M.R., Paiva, S.C.O., Stucchi, E.B. and Flor, J. (2003) New X-Ray Powder Diffraction Data and Rietveld Refinement for Gd_2O_3 Monodispersed Fine Spherical Particles. *Journal of Solid State Chemistry*, **171**, 420-

423. http://dx.doi.org/10.1016/S0022-4596(02)00224-4

[21] Kennedy, B.J. and Avdeev, M. (2011) The Structure of *C*-Type Gd_2O_3: A Powder Neutron Diffraction Study Using Enriched [160]Gd. *Australian Journal of Chemistry*, **64**, 119-121. http://dx.doi.org/10.1071/CH10310

[22] Zachariasen, W.H. (1928) Skrifter utgitt av det Norske Videnskaps Akademi i Oslo 1: Matematisk Naturvidenskapelig Klasse.

[23] Pavlyuk, V.V., Rozycka, S.E., Marciniak, B., Paul B.V. and Dorogova, M. (2011) The Structural, Magnetic, Hydrogenation and Electrode Properties of $REMg_2Cu_{9-x}Ni_x$ Alloys (RE=La, Pr, Tb). *Central European Journal of Chemistry*, **9**, 1133-1142. http://dx.doi.org/10.2478/s11532-011-0099-2

[24] Finkel'shtein, L.D., Samsonova, N.D. and Bazuev, G.V. (1980) Neighboring Structure of X-Ray Absorption in Determination of Europium-Oxygen Average Distances in Compunds with Improper Polyhedrons. *Russian Journal of Inorganic Chemistry*, **25**, 1124-1128.

[25] Glushkova, V.B., Adylov, G.T., Yusupova, S.G., Sigalov, L.H., Kravchinskaya, M.V. and Rakhimov, R.K. (1988) Phase Rations in YO1.5-TbO1.5 and YO1.5-TbOx Systems. *Inorganic Materials*, **24**, 665-669.

[26] Kunzmann, P. and Eyring, L. (1975) On the Crystal Structures of the Fluorite-Related İntermediate Rare-Earth Oxides. *Journal of Solid State Chemistry*, **14**, 229-237. http://dx.doi.org/10.1016/0022-4596(75)90027-4

[27] McCarthy, G.J. (1971) Crystal Data on *C*-Type Terbium Sesquioxide (Tb_2O_3). *Journal of Applied Crystallography*, **4**, 399-400. http://dx.doi.org/10.1107/S0021889871007295

[28] Gasgnier, M., Schiffmacher, G., Caro, P.E. and Eyring, L. (1986) The Formation of Rare Earth Oxides Far from Equilibrium. *Journal of the Less Common Metals*, **116**, 31-42. http://dx.doi.org/10.1016/0022-5088(86)90214-6

[29] Levine, Z.H. and Allan, D.C. (1989) Linear Optical Response in Silicon and Germanium including Self-Energy Effects. *Physical Review Letters*, **63**, 1719-1722. http://dx.doi.org/10.1103/PhysRevLett.63.1719

[30] Philipp, H.R. and Ehrenreich, H. (1963) Optical Properties of Semiconductors. *Physical Review*, **129**, 1550-1560. http://dx.doi.org/10.1103/PhysRev.129.1550